The Effects of Doubling the CO_2 Concentration on the Climate of a General Circulation Model[1]

SYUKURO MANABE AND RICHARD T. WETHERALD

Geophysical Fluid Dynamics Laboratory/NOAA, Princeton University, Princeton, N.J. 08540

(Manuscript received 6 June 1974, in revised form 8 August 1974)

ABSTRACT

An attempt is made to estimate the temperature changes resulting from doubling the present CO_2 concentration by the use of a simplified three-dimensional general circulation model. This model contains the following simplifications: a limited computational domain, an idealized topography, no heat transport by ocean currents, and fixed cloudiness. Despite these limitations, the results from this computation yield some indication of how the increase of CO_2 concentration may affect the distribution of temperature in the atmosphere. It is shown that the CO_2 increase raises the temperature of the model troposphere, whereas it lowers that of the model stratosphere. The tropospheric warming is somewhat larger than that expected from a radiative-convective equilibrium model. In particular, the increase of surface temperature in higher latitudes is magnified due to the recession of the snow boundary and the thermal stability of the lower troposphere which limits convective heating to the lowest layer. It is also shown that the doubling of carbon dioxide significantly increases the intensity of the hydrologic cycle of the model.

1. Introduction

According to the estimate by Machta (1971), the concentration of carbon dioxide in the atmosphere may increase as much as 20% during the latter half of this century as a result of fossil fuel combustion. It has been speculated that an increase in the CO_2 content in the atmosphere may result in the gradual rise of the atmospheric temperature (Callendar, 1949). Plass (1956), Kaplan (1960) and Kondratiev and Niilisk (1960) estimated the increase of the temperature of the earth's surface required to compensate for the increase in the downward terrestrial radiation due to the increase in the CO_2 content in the atmosphere. According to Plass, the doubling or halving of the CO_2 results in a temperature change of $+3.8°C$ or $-3.6°C$, respectively. Kaplan (1960) attempted to improve Plass' estimate by taking into consideration the effect of cloudiness, as well as by improving the computation scheme of radiative transfer. Kondratiev and Niilisk (1960) considered the effect of overlapping between the 15-μm band of CO_2 and the rotation band of water vapor. The magnitudes of the temperature changes estimated by both Kaplan, and Kondratiev and Niilisk are significantly less than those estimated by Plass, indicating the importance of such factors as cloudiness and overlapping between bands in this problem.

[1] A brief description of this study appears on pp. 238–239 of the Study of Man's Impact on Climate (SMIC, 1971).

Möller (1963) reviewed these studies critically and tried to improve these estimates by making a more realistic assumption. According to Möller, the atmosphere tends to restore a certain climatological distribution of relative humidity in response to the change of temperature. The change in surface temperature is accomplished by a change in air temperature, which in turn causes the changes in absolute humidity of air and in the downward terrestrial radiation. The change in absolute humidity also affects absorption of solar radiation and, accordingly, the amount of solar radiation reaching the earth's surface. Taking into consideration all these factors, Möller reevaluated the effect of the increase of carbon dioxide content upon the temperature of the earth's surface. To his surprise, he obtained results which are quite different from those of the earlier studies mentioned above. According to his estimate, an increase in the water vapor content of the atmosphere with rising temperature causes a self-amplifying effect which results in an almost arbitrary temperature change. For example, when the air temperature is around 15°C, the doubling of CO_2 content results in an increase of temperature by as much as 10°C. For other air temperatures, the result may be completely different.

Examining Möller's method, Manabe and Wetherald (1967) felt that it was necessary to take into consideration another physical factor in order to obtain reasonable results. They maintained that the change

in CO_2 content not only affects the flux of net radiation at the earth's surface but also the fluxes of sensible and latent heat from the earth's surface to the atmosphere. In order to find out how the flux of total heat energy depends upon the CO_2 content, it is necessary to take into consideration the heat balance of the atmosphere as well as that of the earth's surface. Therefore, Manabe and Wetherald proposed to use a one-dimensional model of radiative-convective equilibrium to investigate this problem. By comparing the state of radiative-convective equilibrium which was obtained for various CO_2 concentrations, they estimated the dependence of atmospheric temperature upon CO_2 concentration. Following the suggestion of Möller, they incorporated into their model the mechanism of the water vapor greenhouse feedback by assuming a fixed distribution of relative (rather than absolute) humidity in the model atmosphere. Although their results show that the water vapor greenhouse feedback is responsible for increasing the sensitivity of the temperature of the model atmosphere, it does not yield an indefinite result such as that obtained by Möller. They found that the doubling of CO_2 in the air increases the equilibrium temperature of the earth's surface by about 2.3°C provided that no change in cloudiness takes place. Manabe (1971) attempted to improve this result further by replacing his scheme of computing radiative transfer with the method of Rodgers and Walshaw (1966) as modified by Stone and Manabe (1968). In this case, he obtained a somewhat smaller increase of about 1.9°C resulting from the doubling of carbon dioxide content.

Rasool and Schneider (1971) also estimated the thermal effects of a change in the concentration of CO_2 based upon the consideration of the heat balance of the atmosphere. It turned out that the change in surface temperature which they estimated is much smaller than the change obtained by Manabe and Wetherald. According to our more recent studies, a significant part of the difference stems from the following effects:

1) Rasool and Schneider did not take into consideration the fact that the temperature change in the stratosphere has an opposite sign to that in the troposphere.

2) The absorption of solar radiation is altered if the atmospheric temperature and accordingly also the water vapor content changes. This factor was not considered by Rasool and Schneider.

The models of Rasool and Schneider (1971) and Manabe and Wetherald (1967) are globally averaged models. However, the climate of the planet Earth is maintained by the nonlinear coupling between various processes, such as the poleward heat transfer by the atmospheric and oceanic circulations, as well as the vertical heat transfer by radiative transfer and convection. Thus, it is clear that one cannot obtain a definitive conclusion, using a globally averaged model, concerning the effect of an increase in CO_2 upon climate. Recently, Budyko (1969) and Sellers (1969) constructed a very simple model of the atmosphere in which the effects of a poleward heat transport as well as radiative transfer were included although in highly parameterized forms. In addition, they incorporated into their model the following positive feedback mechanism that would tend to enhance the sensitivity of the model climate:

decrease (increase) of atmospheric temperature
→wider (narrower) area of snow cover or ice pack
→larger (smaller) albedo of earth's surface
→decrease (increase) of atmospheric temperature.

By using their model, Budyko and Sellers suggested that the thermal regime of the model atmosphere is highly sensitive to small changes in various parameters, such as the solar constant, when the process of the snow cover feedback is incorporated. Their study suggests that it is important to consider this feedback mechanism for our problem. Since the heat transport by large-scale eddies is parameterized in an extremely simple manner and many idealizations are made in their model, it is clear that we need a better model for a quantitative study of the climatic change resulting from an increase of the amount of CO_2 in the atmosphere.

The present study represents a preliminary attempt to do this by using a three-dimensional general circulation model in which the heat transport by large-scale eddies is computed explicitly rather than by parameterization. The long-term integrations of the model are carried out for two different concentrations of CO_2, i.e., the present and twice the present concentration. By comparing the two quasi-equilibrium states which emerge from these experiments, we will evaluate how the concentration affects the state of the model atmosphere.

It should be noted here that a sensitivity study such as described in this paper is meaningful provided that the following conditions are satisfied.

(i) The model has a stable equilibrium climate.
(ii) An external forcing (such as the doubling of CO_2 concentration) is not large enough to force the model climate out of the stable equilibrium into a markedly different state.

Obviously, it is useful to inquire how large an external forcing is required in order to push the model climate out of stable equilibrium or how the model climate changes thereafter. However, it is not the subject of the present study.

In view of the many simplifications adopted for the construction of the model, the result from this study should not be regarded as a definitive study of this problem. Instead, we are satisfied if this study yields

some valuable insight into the physical factors which control the response of the atmosphere to the change in the carbon dioxide content in the atmosphere.

2. Description of the model

The general circulation model used for this study is essentially the same as that described by Manabe (1969). Therefore, only a brief description of the model is given here.

The model solves the primitive equations on a Mercator projection using an energy conserving form of the finite-difference formulation. The vertical coordinate is defined by pressure normalized by surface pressure. To simulate the effects of subgrid mixing, a nonlinear viscosity is included in the model. The topography adopted is the same as that described by Manabe (1969). Free-slip insulated walls are placed at the equator and at 81.7N, whereas cyclic continuity is assumed for the two meridional boundaries 120° of longitude apart. Grid-point spacing is such that the resolution is approximately 500 km. Nine vertical levels are chosen so that the model can simulate the structure of both the stratosphere and the planetary boundary layer. The computational domain is divided into two equal areas up to 66.5N latitude, continent and "ocean," respectively. From 66.5N to the polar boundary at 81.7N, continent is assumed throughout. A diagram of the computational region is shown in Fig. 1. It should be stressed here that this model does not contain a separate ocean computation. The "ocean" portion is simply considered to be an area of wet land or an area possessing an infinite source of soil moisture for evaporation. The model ocean resembles the actual ocean in the sense that it is wet, but it lacks the effects of heat transport by ocean currents.

The scheme for computing radiative heating and cooling is described by Manabe and Strickler (1964) and Manabe and Wetherald (1967), and computes both solar and longwave radiation fluxes.[2] The distribution of cloudiness is specified from annual mean observations and is a function of latitude and height only. Three atmospheric gases are taken into account, i.e., water vapor, ozone and carbon dioxide. The distribution of water vapor is determined by the prognostic equations of the model or, in other words, the radiative computation is "coupled" with the hydrologic cycle. The spatial distribution of ozone is specified in a manner analogous to clouds. The mixing ratio of carbon dioxide is taken to be constant everywhere. The surface temperature over the continent and the hypothetical ocean is determined from the boundary condition that no heat is stored at the earth's surface, i.e., net fluxes of solar and terrestrial radiation and the turbulent fluxes of sensible and latent heat locally sum to zero.

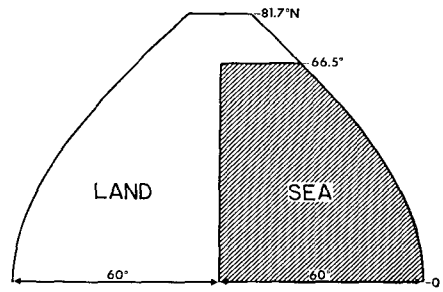

FIG. 1. Diagram illustrating the distribution of continent and "ocean." Cyclic continuity is assumed at the eastern and western ends of the domain.

The prognostic system of water vapor involves the three-dimensional advection of water vapor, evaporation, vertical mixing, nonconvective condensation, and an idealized moist convective adjustment. Over continental surfaces, the depth of snow cover and the amount of soil moisture are based upon detailed balance computations of snow and soil moisture, respectively. In particular, the snow depth is increased by snowfall and depleted by evaporation and snowmelt. The latter quantity is computed from the requirement of the heat balance when conditions for the snowmelt are satisfied. [See Manabe (1969) for further description of the prognostic system of soil moisture and snow.] Differentiation between rain or snow is determined by the temperature at a height of approximately 350 m. If this temperature is equal to less than 0°C, precipitation is in the form of snow; otherwise, it occurs in the form of rain. Over the oceanic region, the area of sea ice is identified as the area where the surface temperature over the ocean is less than −2°C.

For the computation of the heat balance at the earth's surface, it is necessary to know the distribution of surface albedo. It is assumed that the albedo of the soil surface is a function of latitude and that its distribution with latitude is the same as that used by Manabe (1969). The albedos of snow cover and sea ice are assumed to be much larger than the albedo of bare soil. As pointed out in the Introduction, this difference in albedo accounts for the snow cover feedback.

Both snow cover and sea ice are classified into two categories, i.e., permanent and temporary snow cover (sea ice). Different values of albedo are assigned to each category. Referring to the study of Budyko (1956), unstable snow cover and unstable sea ice are assigned an albedo of 0.45 and 0.35, respectively, whereas both permanent snow cover and permanent sea ice are assigned a common albedo of 0.70. The discrimination between the permanent and temporary snow cover (sea ice) is made according to the surface

[2] The model of radiative transfer is adjusted slightly such that it does not contain a systematic bias. For more details, see Appendix A.

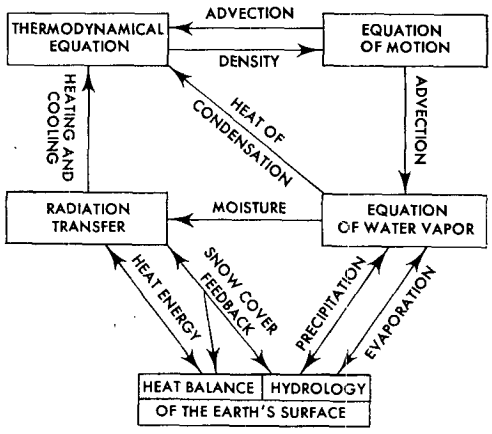

FIG. 2. Box diagram indicating the major components of the model. Arrows represent the links between components.

temperature of snow cover (sea ice). Originally, we intended to assume this critical surface temperature to be —10°C. Because of a mistake in the programming, the value of −25°C was actually used instead of −10°C. This error will have the effect of displacing the permanent ice cap with high albedo further northward (by about 10° latitude) than it would have been otherwise. Therefore, the results presented in this study must be interpreted with this in mind.[3]

In concluding this section, a block diagram, which illustrates the structure of the model, is shown in Fig. 2.

3. Approach toward the equilibrium

As mentioned in the Introduction, the numerical experiments are performed for two different concentrations of CO_2, i.e., the present and twice the present amount. The specific values of mixing ratio chosen for these two cases are 0.456×10^{-3} g kg^{-1} and 0.912×10^{-3} g kg^{-1}, respectively. The climatic effects of this doubling of the CO_2 concentration will be identified next by comparing the two quasi-equilibrium states of the model atmospheres which are obtained by the method described below.

Starting from the initial condition of an isothermal atmosphere at rest, the model is integrated with respect to time over a period of approximately 800 days. One version of the equilibrium climate is thus obtained by averaging over the last 100-day period. In order to reduce the bias in the equilibrium climate resulting from the specific choice of initial conditions, another integration is carried out starting from quite different initial conditions, which are described in Appendix B. The final state of equilibrium is now obtained by averaging the two 100-day mean states.

In order to attain a satisfactory convergence toward statistical equilibrium, it is necessary to carry out the time integration for sufficiently long periods. The degree of convergence obtained by the procedure described above is evident in Fig. 3. This figure shows how the (mass-weighted) mean temperature of the model atmosphere changes with time starting from the two initial conditions. Note that the initial values for the two runs are considerably different from one another, but that they are practically indistinguishable toward the end of the runs. The difference between the two mean temperatures averaged over the last 100 days of each integration is about 0.10°C. For a further discussion of the convergence of the solution, see Appendix B.

4. Doubling of CO_2 concentration

This section deals with the comparison between the two statistical equilibrium states corresponding to the present and twice the present concentration of CO_2. For ease of identification, the case of the present concentration is identified as the "standard" case and that of double concentration as the "$2\times CO_2$" case. Unless we specify otherwise, the results presented here are obtained by taking the average of two time-mean states, which are computed from the last 100-day period of each integration as described in the preceding section.

a. Temperature

The latitude-height distribution of the zonal mean temperature in the model atmosphere with a normal concentration of carbon dioxide is shown in Fig. 4a. According to the comparison between this result and the distribution of observed annual mean temperature,[4] the thermal structure of the model atmosphere generally resembles that of the actual atmosphere. However, the surface temperature in the model tropics is significantly higher than the observed value due to the lack of the poleward transport of heat by ocean currents (see Fig. 5 also). In the lower stratosphere of the model, the zonal mean temperature in middle latitudes is significantly colder than observed. The failure of the model to produce the relatively warm belt in the lower stratosphere of the middle latitudes seems to be a characteristic of the limited domain model which cannot accommodate ultra-long waves (see Manabe, 1969).

Fig. 4b shows the difference in zonal mean temperature between the $2\times CO_2$ and the standard case.

[3] According to Raschke *et al.* (1973), the annual zonal mean planetary albedo near the North Pole does not greatly exceed 50% as deduced from Nimbus 3 satellite data. A surface albedo of 70% according to our calculations at higher latitudes and average cloudiness yields a planetary albedo considerably greater than this or approximately 65%. On the other hand, a surface albedo of 45% under the same conditions yields a planetary albedo of about 55% which is in better agreement with the observations cited above. See Section 4d for further discussion of this subject.

[4] See, for example, Fig. 5.1 of Manabe *et al.* (1965).

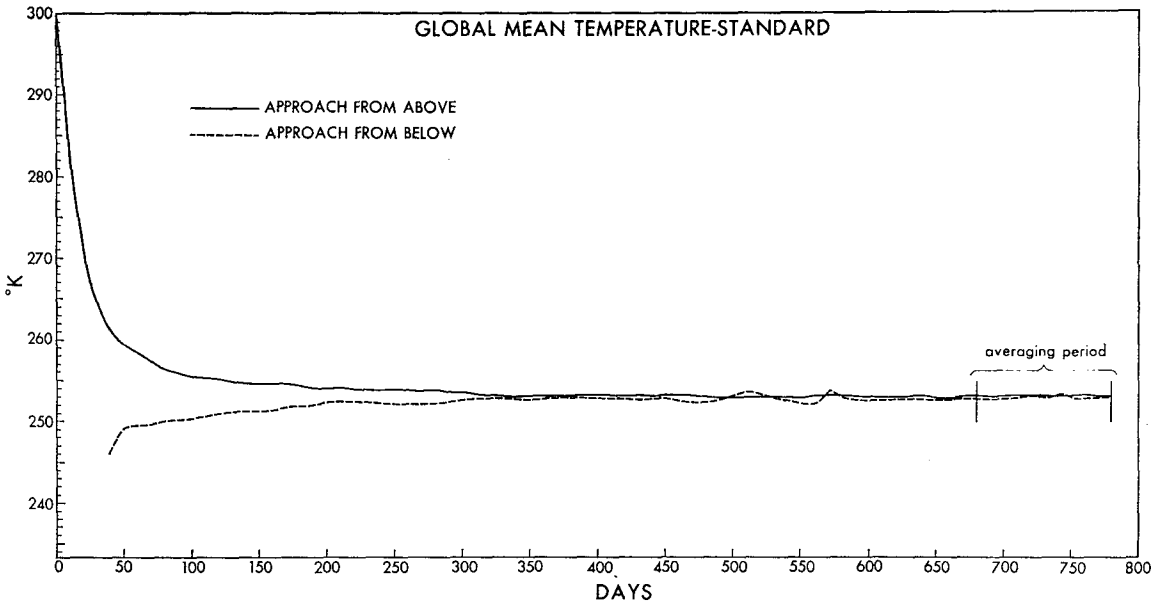

FIG. 3. Time variation of (mass-weighted) mean temperature (K) for the entire period of integration of the two standard runs.

Owing to the increase in the greenhouse effect resulting from the increase in the concentration of CO_2, there is a general warming in the model troposphere. On the other hand, large cooling occurs in the model stratosphere. Qualitatively similar results were obtained by Manabe and Wetherald (1967) in their study of radiative-convective equilibrium of the atmosphere. According to Fig. 4b, the tropospheric warming is most pronounced in the lower troposphere in high latitudes. This large warming is associated with the decrease in the area of snow (or ice) cover, which has a much larger albedo than the soil surface. The increase in downward terrestrial radiation due to the increase in the amount of CO_2 contributes to the decrease in the area of snow cover and, as a result, to the increase in the amount of solar radiation absorbed by the earth's surface. As mentioned above, the warming in high latitudes is confined within a relatively shallow layer next to the earth's surface because the vertical mixing by turbulence is suppressed in the stable layer of the troposphere in polar regions. Therefore, most of the thermal energy involved goes into raising the temperature of this shallow surface layer rather than being spread throughout the entire depth of the troposphere. In short, the effects of suppression of vertical mixing together with those of snowmelt are responsible for the large warming in the polar region. It should be noted here that the maximum increase of temperature right next to the polar boundary is partly due to the recession of the permanent ice cover, which has a larger albedo than the variable snow cover. See Section 4d for further discussion of this subject. In the model tropics, the warming spreads throughout the entire troposphere due to intense moist convection. Accordingly, its magnitude is relatively small as compared with the warming in the polar region.

It should be noted that in low and middle latitudes, the warming is greater in the upper troposphere ($\sim$336 mb) than near the surface. This is due to the fact that the moist convective processes in the model tend to adjust temperatures in a column toward the moist adiabatic lapse rate. Since this lapse rate is more stable in a warmer atmosphere than in a colder atmosphere, the greatest difference in temperature will be found near the top of the moist convective layer. Therefore, the area of maximum tropospheric warming occurs in the upper troposphere instead of near the earth's surface.

As pointed out above, large cooling occurs in the model stratosphere. This is caused by the increase in the emission from the stratosphere to space resulting from the increase in the concentration of CO_2. Since the total amount of CO_2 above a given level decreases with increasing altitude, the absorption of the emission from above also decreases correspondingly. This is one reason why the magnitude of the cooling increases with increasing height in the model stratosphere.

The differences between the distributions of surface air temperature for the two cases are further illustrated by Fig. 5, which shows the latitudinal distributions of zonal mean temperature at the lowest prognostic level (i.e., $\sim$991 mb). In particular, there is a considerable difference between the two temperature curves in higher latitudes, whereas there is a smaller

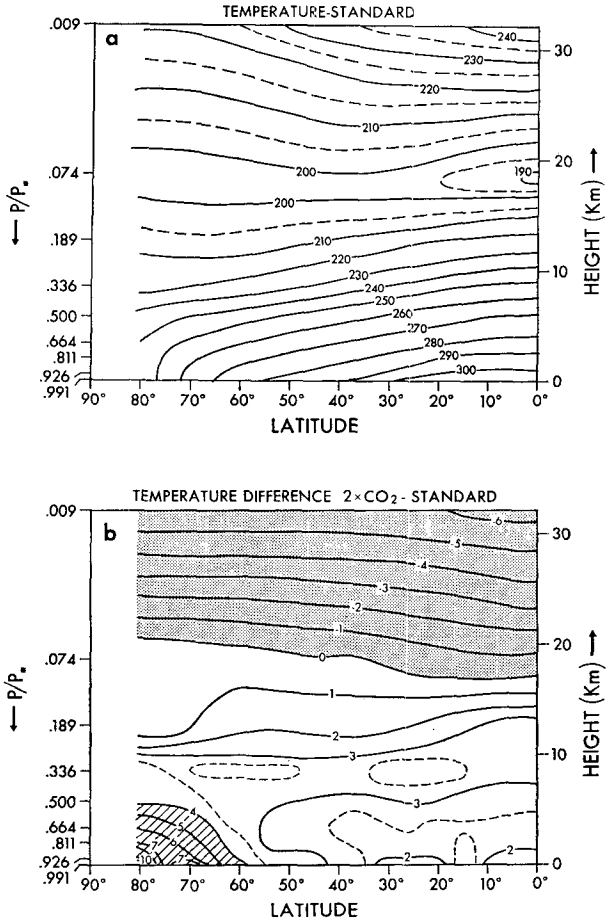

FIG. 4. Latitude-height distribution of the zonal mean temperature (K) for the standard case (a) and of the increase in zonal mean temperature (K) resulting from the doubling of CO_2 concentration (b). Stippling indicates a decrease in temperature.

change at equatorial latitudes. This is consistent with the results shown in Fig. 4b.

In order to evaluate the sensitivity of the mean surface temperature to changes in CO_2 concentration, Table 1 is presented. This table shows the difference of mean surface temperature as a function of CO_2

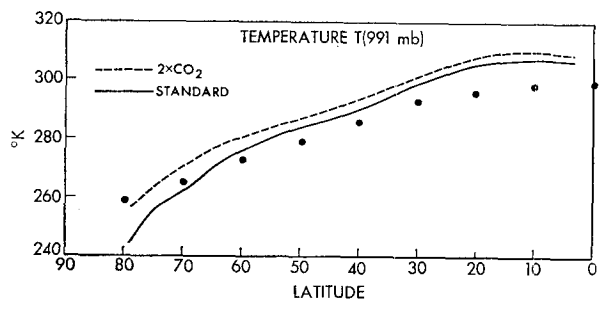

FIG. 5. Zonal mean temperature at the lowest prognostic level (i.e., ~991 mb). Dots indicate the observed distribution of zonal mean surface air temperature (Oort and Rasmusson, 1971).

TABLE 1. Increase in the equilibrium temperature (K) of the earth's surface resulting from the doubling of concentration CO_2. The figure for the G-C (general circulation) model represents the average value over the entire domain.

Change of CO_2 content (ppm)	R-W model	M-W model	G-C model
300 → 600	+1.95	+2.36	+2.93

concentration for both the general circulation model and the associated Manabe and Wetherald (M-W) radiative-convective equilibrium model (1967). (Note that the scheme of computing radiative transfer which is incorporated into the general circulation model is identical to that adopted by M-W.) Also shown, for the sake of comparison, are the corresponding values obtained using a version of the Rodgers-Walshaw (R-W) radiation model (1966) which is modified by Stone and Manabe (1968)[5] and is, in our opinion, a superior model. According to this table, the magnitude of the surface temperature difference is considerably greater for the general circulation model than for the corresponding radiative-convective model by itself. (Note that the general circulation model incorporates the M-W radiation model.) This suggests that the former is more sensitive to changes in CO_2 concentration than the latter. This difference in sensitivity is due, in part, to the snow cover feedback mechanism which is present in the general circulation model but is not accounted for in the radiative-convective equilibrium model. It is of interest to note that the R-W model is slightly less sensitive to CO_2 changes than the M-W model. The reason for this difference in sensitivity between the two models has not been pinpointed at present. Had we used the R-W radiation scheme instead of the M-W scheme, the sensitivity of the general circulation model to the change in CO_2 concentration would be slightly less than what is indicated in the table.

b. Relative humidity

The latitude-height distribution of relative humidity which emerged from the time integration of the model with the standard concentration of carbon dioxide is shown in Fig. 6a. According to the comparison between these results and the observed distribution of zonal mean relative humidity,[6] the relative humidity in the model atmosphere tends to be too high near the earth's surface. However, the model simulates some of the qualitative features of the annual mean

[5] The modified version of the Rodgers-Walshaw model has the following characteristics: 1) it uses the Curtis-Godson 2-parameter approximation instead of scaling approximation; and 2) it computes the contribution of water vapor bands by subdividing them into 19 subintervals and that of the CO_2 15-μm band by subdividing it into 4 subintervals.

[6] See the bottom half of Fig. 7.3 in the paper by Manabe *et al.* (1965).

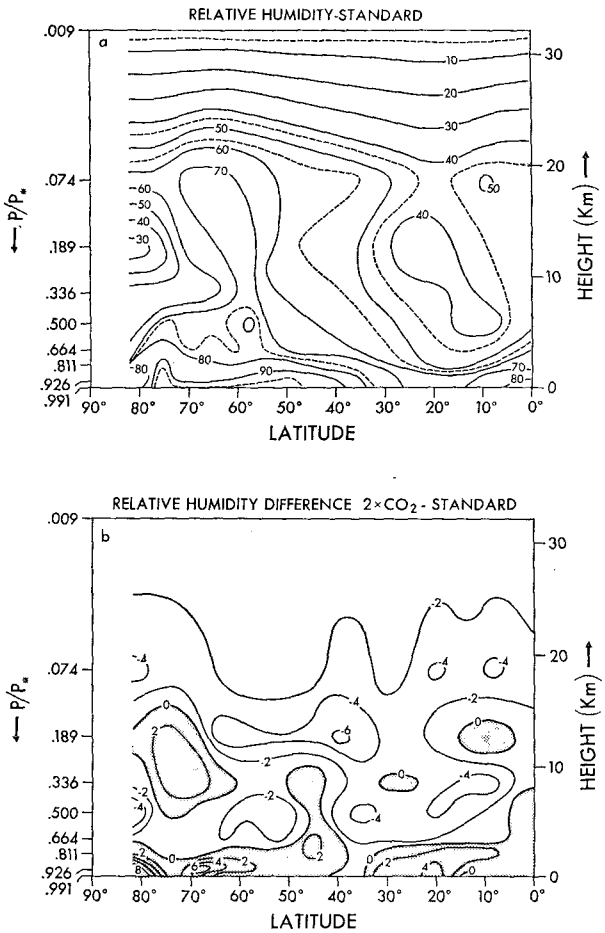

FIG. 6. Latitude-height distribution of zonal mean relative humidity (%) for standard case (a) and of the increase in zonal mean relative humidity resulting from the doubling of CO_2 concentration (b). Stippling indicates an increase of relative humidity.

distributions of relative humidity in the actual atmosphere. For further discussion of relative humidity of the model, see Manabe *et al.* (1965).

Fig. 6b shows the difference in zonal mean relative humidity between the $2\times CO_2$ and the standard case. According to this figure, the pattern is rather irregular. In view of this irregularity, the details of this distribution may not be significant. However, it is probable that the large-scale features of this difference are meaningful. In general, relative humidity increases by a few percent in the lower troposphere (below 700 mb) and decreases in the upper troposphere (above 700 mb). The M-W results suggest that the change of this magnitude in relative humidity does not have very large effects on the state of the thermal equilibrium of the atmosphere. However, it could have changed the cloudiness and affected the temperature of the model atmosphere significantly had the model included the prognostic system of cloudiness. [See, for example, Smagorinsky (1960) for the relationship between cloud amount and relative humidity.] According to M-W and Schneider (1972), cloudiness, particularly low cloud cover, has a very large effect upon the thermal equilibrium of the atmosphere. Therefore, it seems to be necessary to repeat this study later by use of a model with the capability of cloud prediction.

c. Hydrology

Fig. 7 shows the zonal mean precipitation and evaporation rates for the $2\times CO_2$ and the standard cases. For both quantities, the rates for the $2\times CO_2$ case are significantly greater than the corresponding rates for the standard case over most of the region. Averaged over the entire computational domain, the time-mean rate of precipitation is practically equal to that of evaporation. Its value is 0.255 cm day^{-1} for the standard case and 0.275 cm day^{-1} for the $2\times CO_2$ case. This suggests that, within the limits of this study, the general circulation model containing the higher CO_2 content has a significantly more active hydrologic cycle by about 7% than the one with the standard CO_2 content. The greater downward flux of terrestrial radiation resulting from the larger concentration of CO_2 increases the heat energy available for the evaporation from the earth's surface, and thus enhances the intensity of the hydrologic cycle in the model atmosphere. There is another important reason for the intensification of the hydrologic cycle, which is discussed in Section 4e.

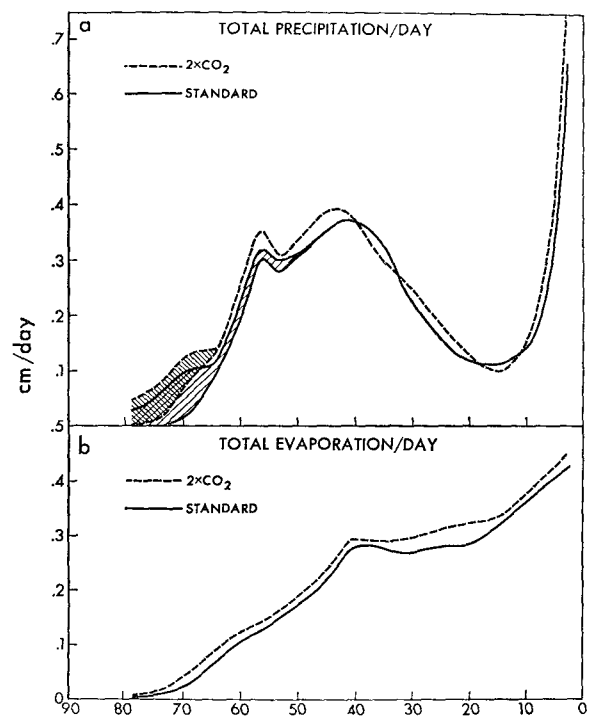

FIG. 7. Zonal mean rates of total precipitation, where shaded areas denote the rates of snowfall (a), and zonal mean rates of evaporation (b).

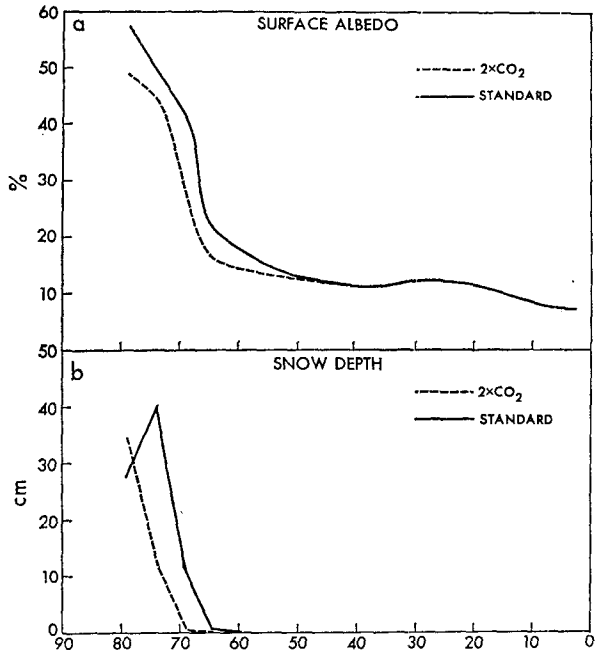

FIG. 8. Zonal mean surface albedo (a) and zonal mean snow depth in water equivalent (b).

Also shown in Fig. 7a are the relative snowfall rates (cross-hatched areas) associated with both cases. Here, it is evident that for the $2\times CO_2$ case, the snowfall rate is less and extends over a considerably smaller latitude area than the snowfall rate for the standard case.

d. Snow cover and albedo

In the preceding discussion, it was stated that a change in the ground albedo (snow cover vs bare soil) was partly responsible for the large warming obtained in higher latitudes. Fig. 8 shows the correspondence between the ground albedo (8a) and snow depth (8b) for the standard and $2\times CO_2$ cases. As expected, the $2\times CO_2$ case is associated with a lower surface albedo and a lesser extent of the snow cover as compared with the standard case. These changes occur mainly in the zone of unstable new snow cover (assigned an albedo of 45%) and at the boundary of the permanent ice cap (assigned an albedo of 70%) which are displaced further northward as the CO_2 concentration is increased. According to Fig. 4b, the area of the largest temperature increase appears to be located near the polar boundary at the surface where the change of ground albedo from 45 to 70% mainly occurs (see the left-hand side of Fig. 8a). There is also a corresponding northward displacement of the zone of maximum snow depth for the $2\times CO_2$ case.[7]

[7] Note that, in both cases, the latitudinal range of the area of snowfall is wider than that of the area of significant snow accumulation. This difference is caused by the effects of snowmelt and sublimation.

It should be recalled here that due to the oversight mentioned in Section 2, the permanent ice cap boundary is displaced poleward by about 10° of latitude and, therefore, neither zonal mean surface albedo curve reaches the maximum value of 70%.

In order to evaluate the consequence of the code error in the snow albedo formulation, the latitudinal distribution of the planetary albedo for the standard case is compared with that of the actual atmosphere, which was determined from the data of the Nimbus 3 satellite by Raschke *et al.* (1973), in Fig. 9. (Here, "planetary albedo" is defined as the reflectivity of the earth-atmosphere system to solar radiation at the top of the atmosphere.) According to this figure, the planetary albedo of the model in middle and high latitudes is either larger than or approximately the same as that of the actual atmosphere, depending on whether the Northern or the Southern Hemisphere is selected for comparison. In other words, the planetary albedo in high latitudes of the model is not smaller than that of the actual atmosphere as one would expect from the nature of the code error. In fact, it is probable that the formulation of the albedos of snow and ice, which are erroneously adopted for this study, may be more realistic than the formulation originally intended. For a better formulation of snow cover albedo, further study is required to iron out the suspected inconsistency between the observed values of surface albedo and those of planetary albedo.

e. Heat balance

The heat balance of the model atmosphere may be summarized by the heat balance diagram shown in Fig. 10. The standard and $2\times CO_2$ cases are depicted by the left-hand and center diagrams, respectively.

According to this figure, the net downward radiation (i.e., the net downward solar radiation minus net upward longwave radiation) increases by about 3.4%, resulting from the doubling of CO_2 content. This is mainly due to the increase in greenhouse effects of carbon dioxide and water vapor. Responding to this increase in net downward radiation, the upward flux of latent heat (i.e., evaporation) increases by as much as 7%, whereas that of sensible heat actually *decreases* by about 8%. This interesting result can be partly explained by the change in the so-called Bowen ratio.[8] The increase in surface temperature due to the doubling of CO_2 raises the saturation vapor pressure at the earth's surface, and thus significantly reduces the Bowen ratio. In other words, evaporation becomes a more effective way of removing heat from the surface of the model earth than the upward flux of sensible

[8] Bowen ratio $=(C_p/L)(T_*-T_a)/(r_*-r_a)$, where the asterisk and a subscripts indicate earth's surface and lowest prognostic level, respectively, C_p the specific heat of air, L the latent heat of evaporation, T the temperature, and r the mixing ratio of water vapor.

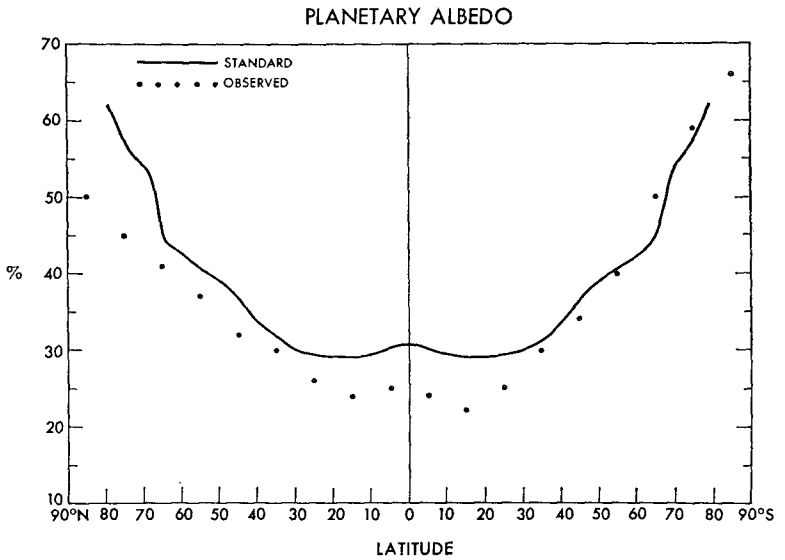

FIG. 9. Solid line: latitudinal distribution of the planetary albedo of the model with the standard concentration of CO_2. The distribution in the Southern Hemisphere represents the mirror image of that in the Northern Hemisphere. Dots: latitudinal distribution of annual mean planetary albedo based upon the data from Nimbus 3 satellite (Raschke *et al.* 1973).

heat. This accounts for why the percentage increase in the rate of evaporation is twice as large as that of net downward radiation. Since the model atmosphere reaches quasi-steady states toward the end of both experiments, this increase in evaporation is almost equal to that in precipitation rate. In short, the doubling of CO_2 increases significantly (by about 7%) the intensity of the hydrologic cycle in the model atmosphere as described in Section 4c.

Another important comparison between the two cases concerns the integrated net solar and longwave radiation at the top of the model atmosphere. According to Fig. 10, net upward longwave radiation increases by $\sim$1% due to the doubling of CO_2. This is because the stratospheric cooling, as well as the increase in the height of the effective source of upward emission caused by the increased CO_2, are overcome by the general warming of the model troposphere. At the same time, there is an increase of about 1% in the intensity of net downward solar radiation. This is due, not only to the lower surface albedo in the polar region, but also to the increased absorption of insolation caused by the increase in both water vapor and carbon dioxide in the model atmosphere.

For the sake of comparison, a similar representation of the actual atmosphere is shown as the right-hand diagram of Fig. 10. The data for this diagram were obtained from Budyko (1963) and London (1957). Despite the idealized land-sea configuration adopted for this study, the agreement between Budyko's results

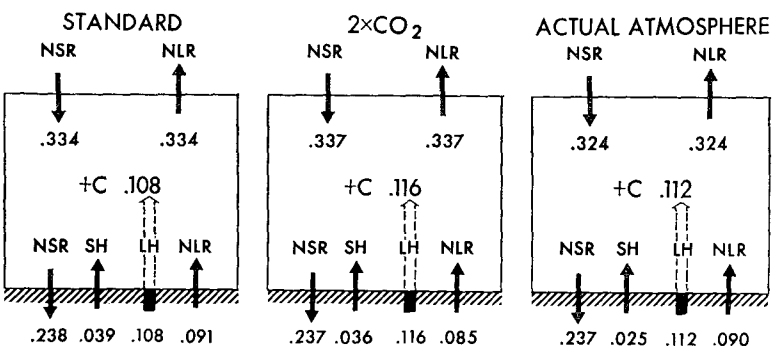

FIG. 10. Box diagrams illustrating area-mean heat balance components (units ly min^{-1}): Left, standard case; middle, $2\times CO_2$ case; right, the actual atmosphere. NLR, net longwave radiation; NSR, net solar radiation; SH, sensible heat flux; LH, latent heat flux. The observed net radiational fluxes are taken from London (1957), and the observed sensible and latent heat fluxes are taken from Budyko (1963).

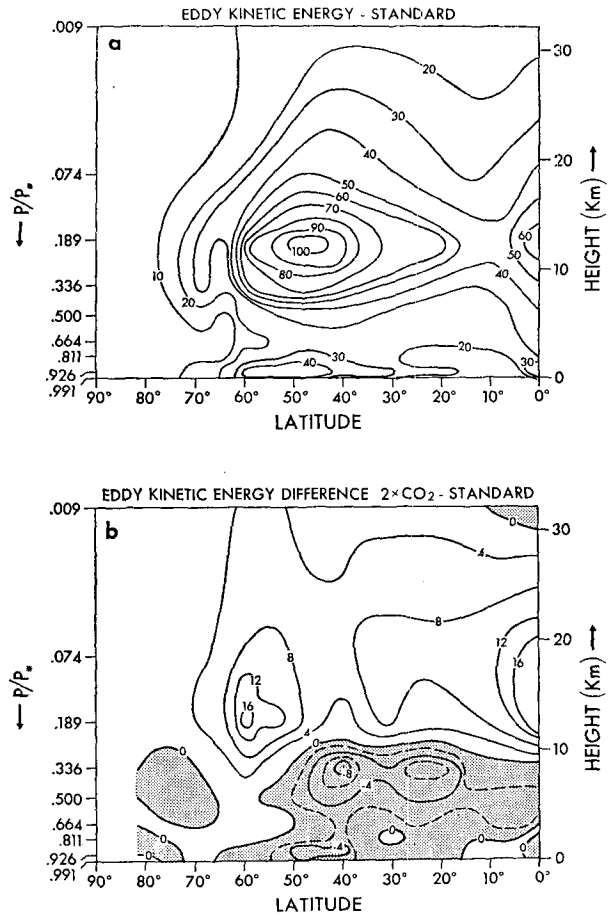

FIG. 11. Latitude-height distribution of zonal mean eddy kinetic energy for the standard case (a) and of the difference in zonal mean eddy kinetic energy resulting from the doubling of the concentration of CO_2 (b). Stippling indicates the region of decrease. Units are in 10^{-3} J cm^{-2} mb^{-1}.

and those computed from the standard case is quite good with perhaps the exception of the sensible heat flux.

f. Eddy kinetic energy

It is of interest to note the effect upon the dynamical processes taking place in the model atmosphere due to the increase of the CO_2 concentration. A measure of these processes is the distribution of eddy kinetic energy[9] which is shown in Fig. 11. Fig. 11a shows the zonal mean latitude-height cross section of eddy kinetic energy for the standard case, and Fig. 11b illustrates the difference of eddy kinetic energy between the $2\times CO_2$ and standard cases. In general, the eddy kinetic energy in the model atmosphere is much lower than that in the actual atmosphere. As pointed out by Manabe *et al.* (1970), this is one of the characteristic features of the model atmosphere with coarse computational resolution of finite differences. According to Fig. 11b, a net decrease of eddy kinetic energy centers between 300 and 500 mb, whereas there is an area of net increase in the layer above the 300-mb level for practically all latitudes. The lower area of maximum net decrease is situated in middle latitudes which approximately coincides with the region of a reduced tropospheric meridional temperature gradient (refer to Fig. 4b). Therefore, the change in meridional temperature gradient, and accordingly, the change in vertical wind shear may be partly responsible for this reduction of eddy kinetic energy. However, the area of net increase in the upper troposphere and lower stratosphere is more difficult to explain. If one compares the zonal mean temperature difference (Fig. 4b) with Fig. 11b, it may be seen that the region of maximum increase of eddy kinetic energy corresponds closely to the level where the static stability decreases the most. Therefore, one may expect a larger generation of eddy kinetic energy for the $2\times CO_2$ case as

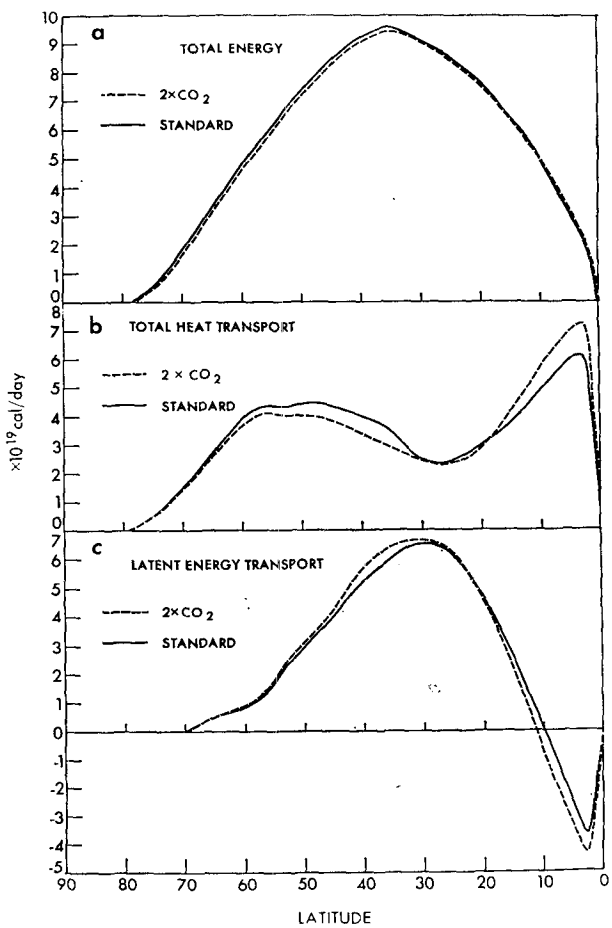

FIG. 12. Poleward transport of total energy ($C_pT+\phi+K+Lr$), a., poleward transport of heat energy ($C_pT+\phi+K$), b., and poleward transport of latent energy (Lr), c.

[9] Here, eddy kinetic energy is defined as the kinetic energy of the component of wind which represents the deviation from the zonal mean wind vector.

compared with the standard case. This may partly explain why the eddy kinetic energy in the upper troposphere and lower stratosphere of the model increases due to the increase in the concentration of CO_2.

g. Poleward transport of energy

One of the important factors which indicate the general activity of the atmospheric circulation is the poleward transport of energy. Fig. 12 shows the poleward transport of total energy ($C_pT+\phi+K+Lr$), heat energy ($C_pT+\phi+K$), and latent energy (Lr) across each latitude circle. Here, T, ϕ, K and r represent temperature, geopotential height, kinetic energy and mixing ratio, respectively; and C_p and L denote the specific heat of air and latent heat of evaporation.

1) HEAT ENERGY.

According to Fig. 12b, the doubling of the concentration of CO_2 in the model atmosphere reduces the poleward transport of heat energy in middle latitudes. This result is consistent with the decrease of the eddy kinetic energy in the lower troposphere where the major portion of heat transport by large-scale eddies is accomplished.

In the model tropics, the opposite situation holds. The poleward heat transport increases slightly due to the doubling of CO_2. Again, this result is consistent with the change in the distribution of precipitation described in Section 4c. The increase in rainfall results from intensification of the Hadley cell which increases the poleward transport of heat energy.

2) LATENT ENERGY.

In middle latitudes of the model, the poleward transport of latent energy (Fig. 12c) increases slightly due to the doubling of CO_2. This increase takes place despite the reduction of lower tropospheric eddy kinetic energy mentioned above. The general increase of the water vapor in the atmosphere associated with the rise of temperature may be responsible for this result.

In low latitudes, the equatorward transport of latent heat for the $2\times CO_2$ case is larger than that for the standard case. Again, the intensification of the Hadley cell mentioned above is mainly responsible for this difference.

3) TOTAL ENERGY.

Fig. 12a indicates that the increase of the concentration of CO_2 results in reduction of the poleward transport of total energy in the model atmosphere over most of the latitudes with the exception of the tropics. However, the magnitude of the change is very small because the change in heat transport is mostly offset by the change in the transport of latent heat.

5. Summary and conclusions

In this study, an attempt is made to analyze the effect of doubling the CO_2 concentration in a highly simplified three-dimensional general circulation model. The main results of this study may be summarized as follows:

1) In general, the temperature of the model troposphere increases resulting from the doubling of the concentration of carbon dioxide. This warming in higher latitudes is magnified two to three times the overall amount due to the effects of snow cover feedback and the suppression of the vertical mixing by a stable stratification. Because of the snow cover feedback mechanism, the overall sensitivity of the three-dimensional model is found to be significantly larger than that of the radiative-convective equilibrium model.

2) The temperature of the model stratosphere decreases because of the larger emission from the stratosphere into space caused by the greater concentration of CO_2. The magnitude of the cooling increases with increasing altitude. Hence, the static stability in the stratosphere tends to decrease.

3) A more active hydrologic cycle is obtained as indicated by the greater rates of total precipitation and evaporation computed in this study. This is due not only to the increase in the flux of downward radiation at the earth's surface, but also to the decrease in the Bowen ratio, resulting from the increase in the saturation vapor pressure for surface temperature. Also obtained is a poleward displacement of snow cover, which is consistent with the increase of surface temperature in high latitudes.

4) An analysis of the eddy kinetic energy indicates an overall reduction of this quantity in the lower troposphere, particularly in middle latitudes. This layer of decrease approximately coincides with the layer of reduced meridional temperature gradient. Conversely, there is an increase of eddy kinetic energy in the upper troposphere and lower stratosphere which corresponds approximately with the height at which the static stability decreases.

In evaluating these results, one should recall that the current study is based upon a model with a fixed cloudiness. As pointed out in Section 4, the results may be altered significantly if we used a model with the capability of predicting cloudiness. Other major characteristics of the model which can affect the sensitivities of the model climate are idealized geography, swamp ocean, and no seasonal variation.

Because of the various simplifications of the model described above, it is not advisable to take too seriously the quantitative aspect of the results obtained in this study. Nevertheless, it is hoped that this study not only emphasizes some of the important mechanisms which control the response of the climate to the change of carbon dioxide, but also identifies the various re-

quirements that have to be satisfied for the study of climate sensitivity with a general circulation model.

Acknowledgments. It is a pleasure to acknowledge J. Smagorinsky, the Director of the Geophysical Fluid Dynamics Laboratory, who has given wholehearted support and encouragement during the course of this research. The very useful comments of I. Held, M. Suarez, A. Oort, C. Leith and M. MacCracken are appreciated. Finally, we would like to thank E. D'Amico, E. Groch, M. Stern and P. Tunison for assisting in the preparation of the manuscript.

APPENDIX A

Adjustment of the Radiation Model

Recently, we have suspected that the model of radiative transfer which is being used at the Geophysical Fluid Dynamics Laboratory (Manabe and Strickler, 1964; Manabe and Wetherald, 1967) has a systematic bias. Incorporated into a general circulation model, it tends to yield a model atmosphere which is significantly colder than the actual atmosphere. Such a bias does not cause serious difficulty in a model with a given distribution of sea-surface temperature as a lower boundary condition because the ocean is assumed to have an infinite heat capacity. However, it can yield unrealistic temperatures for a model in which the temperature of the earth's surface is computed explicitly. In order to eliminate this bias in the present study, the radiative model is adjusted such that the area-mean net flux of radiation at the top of the atmosphere is zero *given the observed distributions of temperature and atmospheric absorbers.* The data used for this adjustment test are taken from the following studies: zonal mean temperature, zonal mean humidity, and average cloudiness from London (1957); and surface albedo from Posey and Clapp (1964). Adopting these data, the net upward flux of radiation at the top of the atmosphere is computed for the four seasons. According to this computation, the model yields a net radiative cooling of the atmosphere as a whole, which confirms our earlier suspicions. In order to obtain a satisfactory balance, the following adjustments are performed even though these adjustments resulted in the choice of less realistic values for the relevant parameters.

(i) The contribution of molecular scattering to the planetary albedo is assumed to be 6% instead of 7%.
(ii) The reflectivity of low cloud to solar radiation is assumed to be 63% instead of 69%.
(iii) High cloud or cirrus is assumed to be fully black with regard to longwave radiation.

When these adjustments are applied, the net radiative flux[10] at the top of the atmosphere becomes -0.0003 ly min^{-1} which is negligible for most practical purposes. This adjusted model is used for all numerical experiments carried out in this study.

[10] Net downward flux of solar radiation minus net upward flux of terrestrial radiation.

APPENDIX B

Reduction of Bias in a Quasi-Equilibrium State

It is stated in Section 2 that, in order to reduce the bias in the equilibrium climate resulting from a particular choice of initial conditions, the experiments are rerun starting from a considerably different initial condition. This second initial condition is illustrated schematically in Fig. B1.

Let $\mathbf{M}_1$ be the entire matrix of fields representing the state of the model atmosphere on the 40th day of the first run. A new matrix of fields $\mathbf{M}_1'$ is then generated such that $\mathbf{M}_1'=2\mathbf{M}_2-\mathbf{M}_1$, or $\mathbf{M}_1'-\mathbf{M}_2 = -(\mathbf{M}_1-\mathbf{M}_2)$, where $\mathbf{M}_2$ represents the final state obtained from the first run. This $\mathbf{M}_1'$ matrix is then used to start the second run. To economize on computer time, we selected day 40 rather than day 1 of the first run as a point in model time for $\mathbf{M}_1$.

A measure of the degree of convergence discussed in Section 2 is the time variation of mean temperature for the two runs corresponding to the standard case (Fig. 3). This convergence can be further illustrated by the distribution of zonal mean temperature difference between the two standard runs averaged over the last 100 days of each experiment, shown in Fig. B2. This figure indicates that the absolute magnitude of the difference is generally less than 1 K except for a small region in the lower stratosphere. These differences were considered to be small enough to allow a sensitivity analysis to be performed. Similar graphs are obtained for the $2\times CO_2$ case, but they differ little, qualitatively, from Figs. 3 and B2 and are, therefore, omitted.

It should be mentioned here that the time integration from the second initial condition may lead to a quasi-equilibrium state which is considerably different from the one obtained from the first integration. Such a situation did not occur during the course of the present effort. However, there are indications that the general circulation model used here has more than one stable equilibrium climate for a given set of external

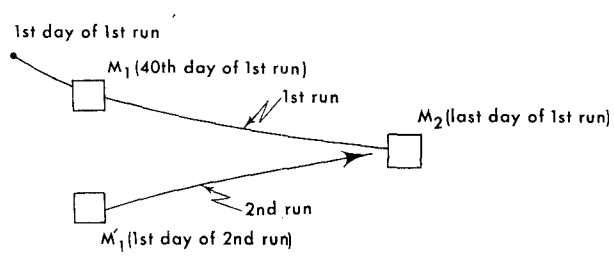

FIG. B1. Diagram of the procedure used to generate the initial condition for the second run in each case. See main text for further explanation.

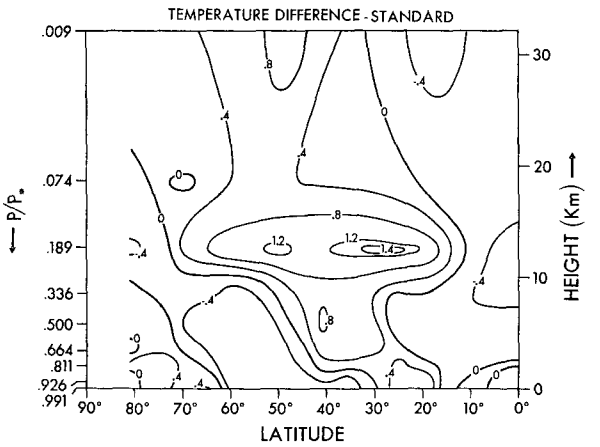

FIG. B2. Latitude-height distribution of the zonal mean temperature difference (K) between the two standard runs.

parameters, such as the solar constant (see, for example, Budyko, 1969). This subject will be discussed in more detail in a future study as it is beyond the scope of the present investigation.

REFERENCES

Budyko, M. I., 1956: *The Heat Balance of the Earth's Surface.* 255 pp. (English transl., N. A. Stepanova, 1958, OTS.)

——, 1963: *Atlas of the Heat Balance of the Earth.* Moscow, Gl. Geofiz. Observ., 69 pp.

——, 1969: The effect of solar radiation variations on the climate of the Earth. *Tellus,* **21,** 611–619.

Callendar, G. S., 1949: Can carbon dioxide influence climate? *Weather,* 4, 310–314.

Kaplan, L. D., 1960: The influence of carbon dioxide variation on the atmospheric heat balance. *Tellus,* **12,** 204–208.

Kondratiev, K. Ya., and H. I. Niilisk, 1960: On the question of carbon dioxide heat radiation in the atmosphere. *Geofis. Pura Appli.,* **46,** 216–230.

London, J., 1957: A study of the atmospheric heat balance. Final Report, Contract AF19(122)-165, New York University, 99 pp.

Machta, L., 1971: The role of the oceans and the biosphere in the carbon dioxide cycle. Nobel Symposium 20, Gothenburg, Sweden.

Manabe, S., 1969: Climate and the ocean circulation: I. The atmospheric circulation and the hydrology of the earth's surface. *Mon. Wea. Rev.,* **97,** 739–774.

——, 1971: Estimates of future change of climate due to the increase of carbon dioxide concentration in the air. *Man's Impact on the Climate,* W. H. Matthews, W. W. Kellogg, and G. D. Robinson, Eds., The MIT Press, 249–264.

——, J. Smagorinsky, J. L. Holloway, Jr., and H. M. Stone, 1970: Simulated climatology of a general circulation model with a hydrologic cycle: III. Effects of increased horizontal computational resolution. *Mon. Wea. Rev.,* **98,** 175–212.

——, —— and R. F. Strickler, 1965: Simulated climatology of a general circulation model with a hydrologic cycle. *Mon. Wea. Rev.,* **93,** 769–798.

——, and R. F. Strickler, 1964: Thermal equilibrium of the atmosphere with a convective adjustment. *J. Atmos. Sci.,* **21,** 361–385.

——, and R. T. Wetherald, 1967: Thermal equilibrium of the atmosphere with a given distribution of relative humidity. *J. Atmos. Sci.,* **24,** 241–259.

Möller, F., 1963: On the influence of changes in the CO_2 concentration in air on the radiation balance of the earth's surface and on the climate. *J. Geophys. Res.,* **68,** 3877–3886.

Oort, A. H., and E. M. Rasmusson, 1971: Atmospheric circulation statistics. NOAA Prof. Paper 5, 323 pp.

Plass, G. N., 1956: The carbon dioxide theory of climatic change. *Tellus,* **8,** 140–154.

Posey, J. W., and P. F. Clapp, 1964: Global distribution of normal surface albedo. *Geofis. Intern.,* **4,** 33–48.

Raschke, E., T. H. Vonder Haar, W. R. Bandeen and M. Pasternak, 1973: The annual radiation balance of the earth-atmosphere system during 1969–70 from Nimbus 3 measurements. *J. Atmos. Sci.,* **30,** 341–364.

Rooasl, S. I., and S. H. Schneider, 1971: Atmospheric carbon dixoide and aerosols: Effects of large increases on global climate. *Science,* **173,** 138–141.

Rodgers, C. D., and C. D. Walshaw, 1966: The computation of infra-red cooling rate in planetary atmospheres. *Quart. J. Roy. Meteor. Soc.,* **92,** 67–92.

Schneider, S. H., 1972: Cloudiness as a global climatic feedback mechanism: The effects on the radiation balance and surface temperature of variations in cloudiness. *J. Atmos. Sci.,* **29,** 1413–1422.

Sellers, W. D., 1969: A global climatic model based on the energy balance of the earth-atmosphere system. *J. Appl. Meteor.,* **8,** 392–400.

Smagorinsky, J., 1960: On the dynamical prediction of large-scale condensation by numerical methods. *Physics of Precipitation,* Monog. No. 5, Amer. Geophys. Union, 71–78.

SMIC, 1971: *Inadvertent Climate Modification.* Report of the Study of Man's Impact on Climate, The MIT Press, 308 pp.

Stone, H. M., and S. Manabe, 1968: Comparison among various numerical models designed for computing infrared cooling. *Mon. Wea. Rev.,* **96,** 735–741.